PHYSICAL REVIEW B **95**, 201407(R) (2017)

Detecting topological invariants in chiral symmetric insulators via losses

Tibor Rakovszky,[1,2] János K. Asbóth,[3] and Andrea Alberti[4]
[1]*Max-Planck-Institut für Physik komplexer Systeme, Nöthnitzer Strasse 38, D-01187 Dresden, Germany*
[2]*Technische Universität München, D-85747 Garching, Germany*
[3]*Institute for Solid State Physics and Optics, Wigner Research Centre for Physics, Hungarian Academy of Sciences, P.O. Box 49, H-1525 Budapest, Hungary*
[4]*Institut für Angewandte Physik, Universität Bonn, Wegelerstrasse 8, D-53115 Bonn, Germany*
(Received 14 December 2016; published 9 May 2017)

We show that the bulk winding number characterizing one-dimensional topological insulators with chiral symmetry can be detected from the displacement of a single particle, observed via losses. Losses represent the effect of repeated weak measurements on one sublattice only, which interrupt the dynamics periodically. When these do not detect the particle, they realize negative measurements. Our repeated measurement scheme covers both time-independent and periodically driven (Floquet) topological insulators, with or without spatial disorder. In the limit of rapidly repeated, vanishingly weak measurements, our scheme describes non-Hermitian Hamiltonians, as the lossy Su-Schrieffer-Heeger model of Rudner and Levitov, [Phys. Rev. Lett. **102**, 065703 (2009)]. We find, contrary to intuition, that the time needed to detect the winding number can be made shorter by decreasing the efficiency of the measurement. We illustrate our results on a discrete-time quantum walk, and propose ways of testing them experimentally.

DOI: 10.1103/PhysRevB.95.201407

Topological insulators [1] are materials whose bulk is gapped, and is characterized by a topological invariant. Depending on the dimensionality of the system and the discrete symmetries it possesses, this invariant can be a Chern number, a winding number, or some other mathematical index [2,3]. The bulk invariant predicts a number of robust low-energy eigenstates at the edges via the so-called bulk-boundary correspondence [4,5]. In one dimension, these are bound states at the ends of the topological insulator wire. The energy of these states is protected against perturbations due to either particle-hole symmetry, as for the Majorana fermions [6] which might be used to store qubits, or to chiral (sublattice) symmetry, as for bound states at domain walls in polyacetylene molecules [7]. Hence, bulk topological invariants control the robust properties of topological insulators.

Of special interest are experiments implementing topological insulators with artificial matter setups, where bulk topological invariants can not only be inferred from the presence of edge states, but also measured directly [8]. Recently, such experiments have been performed using cold atoms in optical lattices [9–14], and using light [15–17] or microwaves [18] in photonic crystal-like structures. These setups often employ periodic driving as a tool to engineer topological phases. Topological invariants are detected by measuring the displacement of a cloud of particles [9,10], or by interferometric schemes [19]. Alternatively, the topological invariant can be observed by attaching leads to the system, and measuring the reflection amplitudes for scattering off the bulk [20–23]. This last approach has recently been applied to detect winding numbers in a one-dimensional quantum walk, an ideal system for periodically driven topological insulators [24].

Topological invariants can also appear in non-Hermitian systems, as predicted by Rudner and Levitov [25], and recently realized experimentally [16]. In that scheme, the Su-Schrieffer-Heeger (SSH) [7,26] model—a nearest-neighbor-hopping Hamiltonian with topological invariants due to chiral symmetry—is modified by adding losses to every second site. The average distance traveled by a particle, initialized on a nonlossy site, before it is lost, is an integer coinciding with the winding number of the original SSH model. However, whether a similar correspondence holds for all chiral symmetric systems in one dimension, has so far remained an open question.

In this Rapid Communication, we show that the expected displacement of a single particle, measured through losses, is given by the bulk topological invariant for any chiral symmetric one-dimensional topological insulator, even in the presence of periodic driving, with or without disorder. Our approach is formulated in the language of periodically driven systems, but by including weak measurements we are also able to cover the case of time-independent multiband Hamiltonians. Note that we use losses to detect topological invariants of the unitary dynamics—unlike other work where topological invariants are engineered through dissipation [27,28].

The setup. We consider one-dimensional lattice systems of noninteracting particles. To describe the state of a single particle we use position eigenstates $|x,c\rangle$, where $x = 1,\ldots,L$ denote the unit cells and $c = 1,\ldots,2N$ are the states forming a basis of a single unit cell. These can be $2N$ different sites, but can also be regarded as $2N$ internal states of the particle [29].

The dynamics is given by a periodically driven Hamiltonian $\hat{H}(t) = \hat{H}(t+T)$. This includes time-independent systems, where T is arbitrary. The time evolution during a whole driving period is described by the unitary operator $\hat{U} = \mathbb{T}e^{-i\int_0^T dt\,\hat{H}(t)}$, where $\mathbb{T}$ denotes time ordering.

It is useful to think of the dynamics in terms of a time-independent *effective Hamiltonian* $\hat{H}_{\rm eff}$, defined by

$$\hat{U} = e^{-i\hat{H}_{\rm eff}T}. \tag{1}$$

The eigenvalues of $\hat{H}_{\rm eff}$, called *quasienergies* and denoted E_n, are periodic with period $2\pi/T$ and can be chosen to lie in the interval $E_n \in [-\pi/T,\pi/T)$. The corresponding eigenstates

are stationary states of the discrete-time evolution that only acquire a phase e^{-iE_nT} during a full cycle. Note that for time-independent systems, the effective Hamiltonian and the usual Hamiltonian coincide. In the following, we use dimensionless energy $\varepsilon_n = E_nT$.

Chiral symmetry and winding number. To enable the system to have nontrivial topological phases, we need to impose some constraint on it, which in this work is *chiral symmetry*. Chiral symmetry for lattice Hamiltonians is also known as sublattice symmetry, since it can be defined by first grouping all internal states into two sets, the *sublattices* A and B. We define these by projectors

$$\hat{P}_A = \sum_{x\in\mathbb{Z}}\sum_{a=1}^{N} |x,a\rangle\langle x,a|, \quad \hat{P}_B = \hat{1} - \hat{P}_A, \tag{2}$$

where $\hat{1}$ is the identity. Chiral symmetry means that the effective Hamiltonian has no matrix elements between states on the same sublattice [30], i.e.,

$$\hat{\Gamma}\hat{H}_{\text{eff}}\hat{\Gamma} = -\hat{H}_{\text{eff}} \quad \text{for } \hat{\Gamma} = \hat{P}_A - \hat{P}_B. \tag{3}$$

The chiral symmetry operator $\hat{\Gamma}$ acts on each unit cell separately and satisfies $\hat{\Gamma}^{-1} = \hat{\Gamma}^\dagger = \hat{\Gamma}$.

An immediate consequence of chiral symmetry is that the eigenstates come in pairs $\{|n\rangle, \hat{\Gamma}|n\rangle\}$, with quasienergies $\{-\varepsilon_n, \varepsilon_n\}$. We will use the projectors onto the upper and lower half of the spectrum,

$$\hat{Q}_- = \sum_{-\pi\leqslant\varepsilon_n\leqslant 0} |n\rangle\langle n|, \quad \hat{Q}_+ = \hat{\Gamma}\hat{Q}_-\hat{\Gamma}. \tag{4}$$

Chiral symmetry allows the system to have nontrivial bulk topological phases. These are characterized by an integer winding number, defined in its most general form [31] as

$$\nu = -\frac{1}{L}\text{Tr}\,\{\hat{P}_B\hat{Q}\hat{P}_A\,[\hat{X}, \hat{P}_A\hat{Q}\hat{P}_B]\}, \tag{5}$$

where $\hat{X} = \sum_{x\in\mathbb{Z}}\sum_{c=1}^{2N} x|x,c\rangle\langle x,c|$ is the position operator, and $\hat{Q} = \hat{Q}_+ - \hat{Q}_-$ is the flatband limit of the (effective) Hamiltonian, defined in terms of the projectors in Eq. (4). In the presence of translational invariance, the above formula for the winding number reduces to its usual definition in quasimomentum space. However, the real-space formula for ν is also valid for disordered systems. Physically, it measures the difference of the electric polarizations of the two sublattices [31].

Weak partial measurement after each period. To detect the winding number, we initialize a single particle on a site on sublattice A, then apply the unitary $\hat{U}$ repeatedly, with each application followed by a partial position measurement. We call this a *partial measurement*, because it measures position only on sublattice B, while avoiding any interaction with the sites of sublattice A. The measurement operation is parametrized by its efficiency $0 < p_M \leqslant 1$. *Weak measurements* ($p_M < 1$) can be realized by coupling the sites of sublattice B to initially unoccupied ancillary sites for a fixed, short time, and then measuring the occupation of the ancillary sites, as shown in Fig. 1. The measurement can yield a positive result, with conditional probability p_M, in which case we detect the position x of the particle and halt observing its quantum evolution. If the measurement returns with a negative result—*a negative measurement*—then we continue with the next unitary driving cycle, followed by the next measurement, and repeat this procedure until a successful detection occurs.

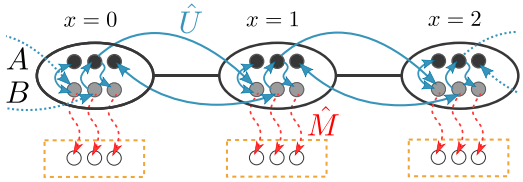

FIG. 1. Weak measurement of position on one sublattice only, represented by the operator $\hat{M}$, following each unitary step $\hat{U}$. First, sites of sublattice B (light gray circles) are coupled (red dashed lines) for a fixed time to ancillary sites. Then, the population of each ancillary site is measured. If all ancillary sites are found empty, we have a negative measurement, and the next unitary step follows. The blue arrows represent matrix elements of the effective Hamiltonian $\hat{H}_{\text{eff}}$.

A practical tool to treat such repeat-until-detection quantum dynamics is the *conditional wave function*. To define it, we first introduce the linear but nonunitary operator $\hat{M}$, representing the effect of a negative measurement on the wave function, as

$$\hat{M} = \hat{P}_A + \sqrt{1-p_M}\,\hat{P}_B. \tag{6}$$

The conditional wave function after j driving cycles but before the jth measurement is

$$|\tilde{\Psi}(t = jT)\rangle = \hat{U}[\hat{M}\hat{U}]^{j-1}|\Psi(0)\rangle \quad \text{for } j \in \mathbb{N}. \tag{7}$$

The norm $\langle\tilde{\Psi}(jT)|\tilde{\Psi}(jT)\rangle$ is the probability that the particle was not detected during the first $j-1$ measurements.

By allowing for weak measurements, with $p_M < 1$, we also cover the case of nondriven, time-independent systems, as in Ref. [25]. There, the chiral symmetric Hamiltonian $\hat{H}$ is modified by an imaginary term describing losses,

$$\hat{H} \to \hat{H} - i\frac{\gamma}{2}\hat{P}_B, \tag{8}$$

where γ is a decay rate. Trotterization of the corresponding time evolution is equivalent to Eq. (7) in the limit $T \to 0$, with $p_M = \gamma T$ and $\hat{U} = e^{-i\hat{H}T}$.

Winding number from average displacement. We are interested in the displacement of the particle and the *dwell time*—the time it spends in the system before it is detected—averaged over many repetitions of the experiment with the same initial state $|x,a\rangle$. The probability of detecting the particle in $|y,b\rangle$ after j steps is

$$s_{(x,a)\to(y,b)}(j) = p_M|\langle y,b|\hat{U}[\hat{M}\hat{U}]^{j-1}|x,a\rangle|^2. \tag{9}$$

We define the average displacement and dwell time as

$$\langle\Delta x\rangle_{(x,a)} \equiv \sum_{j\in\mathbb{Z}^+}\sum_{y=1}^{L}(y-x)\sum_{b=N+1}^{2N} s_{(x,a)\to(y,b)}(j), \tag{10}$$

$$\langle t\rangle_{(x,a)} \equiv T\sum_{j\in\mathbb{Z}^+}\sum_{y=1}^{L} j\sum_{b=N+1}^{2N} s_{(x,a)\to(y,b)}(j). \tag{11}$$

To get a general result, valid for arbitrary N and for spatial disorder, we need to average over all states on sublattice A

where the particle is initially prepared. We define these double-averaged quantities as

$$\langle\langle \Delta x \rangle\rangle = \frac{\sum_{x,a} \langle \Delta x \rangle_{(x,a)}}{NL}, \quad \langle\langle t \rangle\rangle = \frac{\sum_{x,a} \langle t \rangle_{(x,a)}}{NL}. \tag{12}$$

Note that for a large, disordered sample, averaging over all initial sites is expected to give the same result as averaging over different disorder realizations. Note also that for translationally invariant systems $\langle \Delta x \rangle_{(x,a)}$ and $\langle t \rangle_{(x,a)}$ are independent of the initial position, and in this case the averaging over x can be omitted.

To compute $\langle\langle \Delta x \rangle\rangle$ and $\langle\langle t \rangle\rangle$, we write the conditional wave function as

$$\hat{U}[\hat{M}\hat{U}]^{j-1}|x,a\rangle = \sum_n \left[\alpha_n^{(x,a)}(j)|A\rangle_n + \beta_n^{(x,a)}(j)|B\rangle_n\right], \tag{13}$$

where the states $|A\rangle_n = (|n\rangle + \hat{\Gamma}|n\rangle)/\sqrt{2}$ and $|B\rangle_n = (|n\rangle - \hat{\Gamma}|n\rangle)/\sqrt{2}$ have support on sublattices A and B, respectively, and the sum is taken over the lower half of the spectrum. The coefficients evolve in time as

$$\alpha_n(j+1) = \alpha_n(j)\cos\varepsilon_n - i\beta_n(j)\sqrt{1-p_M}\sin\varepsilon_n, \tag{14a}$$

$$\beta_n(j+1) = \beta_n(j)\sqrt{1-p_M}\cos\varepsilon_n - i\alpha_n(j)\sin\varepsilon_n, \tag{14b}$$

with indices (x,a) omitted, since these only appear in the initial condition $\alpha_n^{(x,a)}(0) = \sqrt{2}\langle n|x,a\rangle$. Note that $\beta_n^{(x,a)}(0) = 0$ since the initial state has support on sublattice A. We read off from Eq. (14) that for modes at quasienergies $\varepsilon_n = 0$ or $\varepsilon_n = \pi$ the coefficient $\alpha_n^{(x,a)}(j)$ remains constant in time. Therefore, these are dark states of the lossy dynamics and if the particle has some initial overlap with them, then it has a finite probability of staying in the system forever.

To compute the averages defined in Eqs. (10) and (11) we need the coefficients $\beta_n^{(x,a)}(j)$, which can be obtained by solving Eq. (14), as we show in the Supplemental Material [32]. Substituting the result into Eqs. (12) allows one to perform the sum in Eq. (10) over the discrete time j (assuming that there are no dark states in the spectrum). We thus obtain a compact formula for the double-averaged displacement (derivation in the Supplemental Material [32]),

$$\langle\langle \Delta x \rangle\rangle = -\frac{2}{NL}\mathrm{Tr}\,\{\hat{X}\hat{\Gamma}\hat{Q}_-\}. \tag{15}$$

Note that $\hat{X}\hat{\Gamma} = \hat{P}_A\hat{X}\hat{P}_A - \hat{P}_B\hat{X}\hat{P}_B$ is the difference of the projections of the position operator—i.e., electric polarization—onto the two sublattices. Thus, the above formula is clearly related to the sublattice polarization of Eq. (5). Indeed, after some further algebraic manipulations, we find

$$\langle\langle \Delta x \rangle\rangle = \nu/N. \tag{16}$$

This is our main result that relates the average displacement of a single particle in the lossy system to the winding number associated with the unitary time evolution. It is valid in the same form for static systems, where position is measured via losses as per Eq. (8). Note that to apply either Eq. (5) or Eq. (15) to a finite system with periodic boundary conditions, one has to use an appropriately modified definition of the position operator [33,34].

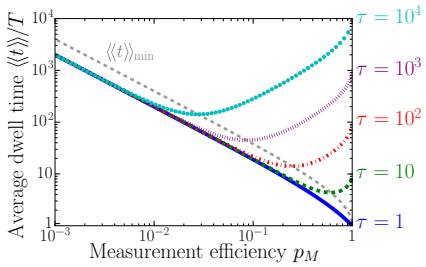

FIG. 2. Plot of the formula (18) for the double-averaged dwell time $\langle\langle t \rangle\rangle$ as a function of the measurement efficiency p_M, for different values of the quantity τ defined in Eq. (17). The gray dashed line shows the minimal average dwell time, obtained by substituting Eq. (19) for different τ. Due to the quantum Zeno effect, $\langle\langle t \rangle\rangle|_{p_M=1} = T\tau$ can be much larger than $\langle\langle t \rangle\rangle|_{\min}$.

Dwell time and quantum Zeno effect. We also find compact formulas for the average dwell time using Eqs. (13) and (14). We detail the derivation in the Supplemental Material [32], and just discuss the results here. First, for strong measurements, $p_M = 1$, the average dwell time can be expressed, in the thermodynamic limit of $L \to \infty$, using the density of states $\rho(\varepsilon)$ as

$$\langle\langle t \rangle\rangle|_{p_M=1} = \frac{T}{N}\int_{\varepsilon=0}^{\pi} \frac{\rho(\varepsilon)}{\sin^2\varepsilon} d\varepsilon \equiv T\tau, \tag{17}$$

where we introduced the shorthand τ for the integral. For weak measurements, this result is modified as

$$\langle\langle t \rangle\rangle = T\left[\frac{p_M}{\left(1+\sqrt{1-p_M}\right)^2}\tau + \frac{2\sqrt{1-p_M}}{p_M}\right]. \tag{18}$$

The average dwell time can become long, or even diverge, in the presence of almost-dark states: In Eq. (17) the integral is dominated by states near $\varepsilon \approx 0$ and $\varepsilon \approx \pi$. These states can occur not only near the topological phase transition but also due to strong disorder. For these states the transition amplitude from sublattice A to B during a single step is infinitesimal. As a consequence, repeatedly measuring the particle's presence on sublattice B can prevent it from ever occupying it, similarly to the well-known quantum Zeno effect.

A counterintuitive way to speed up the measurement process is to *decrease* the measurement efficiency p_M. As the first term in Eq. (18) shows, for $p_M \approx 1$, decreasing p_M decreases the dwell time, in close analogy with the quantum Zeno effect. The price to pay for weak measurements is the second term of Eq. (18), which diverges in the limit $p_M \to 0$ as $\langle\langle t \rangle\rangle \propto 1/p_M$. Hence, there is an optimal value of p_M that minimizes $\langle\langle t \rangle\rangle$, given by

$$p_M^* = 2\,\frac{\tau\sqrt{2\tau-1} - (2\tau-1)}{(\tau-1)^2}. \tag{19}$$

For $\tau \gg 1$, this optimal choice of $p_M = p_M^* \approx \sqrt{8/\tau}$ reduces the time needed to perform the measurement from $T\tau$ to $\langle\langle t \rangle\rangle|_{\min} \approx T\sqrt{2\tau}$, which is a speedup by a factor of $O(\sqrt{\tau})$. These results are illustrated in Fig. 2.

Translating our results for the dwell time to the nondriven case of Eq. (8), where γ is the loss rate, we find

$$\langle\langle t\rangle\rangle = \frac{\gamma \mathrm{t}^2}{4} + \frac{2}{\gamma}, \quad \mathrm{t}^2 \equiv \frac{1}{N}\int_0^\infty \frac{\rho(E)}{E^2} dE. \tag{20}$$

The quantum Zeno-like effect applies here, too. The integral can diverge due to dark and almost-dark states at $E \approx 0$. The optimal choice of the decay rate is $\gamma = \sqrt{8}/\mathrm{t}$, when the two terms of Eq. (20) are equal. In this case, $\langle\langle t\rangle\rangle = \sqrt{2}\,\mathrm{t}$. For the translationally invariant lossy SSH model of Ref. [25], with staggered hopping amplitudes v and v', we find $\mathrm{t} = |v^2 - v'^2|^{-1/2}$, whereby for $v \approx v'$ we obtain $\langle\langle t\rangle\rangle \propto 1/|v - v'|$ as in Ref. [25]. We note that also the usual quantum Zeno effect shows up here: In the limit $\gamma \to \infty$, the measurement process slows down instead of speeding up, with the dwell time diverging as $\langle\langle t\rangle\rangle \propto \gamma$.

Experimental proposal. Our results could be tested using a discrete-time quantum walk—a quantum particle with internal states moving in discrete steps on a one-dimensional lattice. These are periodically driven quantum systems where the effective Hamiltonian cannot be simply obtained perturbatively from the time-dependent Hamiltonian [35]; moreover, they have the advantage of realizing chiral symmetry exactly, a condition which is hard to guarantee in other lattice setups with nonvanishing long-range couplings [17]. In the past, they have been realized using trapped ions [36], cold atoms in optical lattices [37,38], pulses of light [39–43], and most recently using superconducting devices [44,45]. In particular, ultracold atoms trapped in polarization-synthesized optical lattices [46] are ideal candidates to test our results. We have recently demonstrated that negative measurements of the atom's position can be realized using long spin-selective shift operations [38,47]. The spatial distribution of the removed atoms can be recorded via fluorescence imaging [48] after the last step.

To provide a numerical example, we choose the split-step quantum-walk protocol [49], which hosts a variety of topological phases. We consider $2N = 2$ internal states, denoted by $|\uparrow\rangle$ ($c = 1$) and $|\downarrow\rangle$ ($c = 0$), which we refer to as spin. The operator describing the unitary evolution of a single step of the walk is defined as

$$\hat{U}(\theta_1,\theta_2) = \hat{R}(\theta_1/2)\hat{S}_\downarrow \hat{R}(\theta_2)\hat{S}_\uparrow \hat{R}(\theta_1/2), \tag{21}$$

where $\hat{R}(\theta)$ rotates the spin around the y axis by an angle $\theta(x)$, depending in general on site x, and $S_\uparrow$ ($S_\downarrow$) shifts the particle by $+1$ (-1) site if the internal state is $|\uparrow\rangle$ ($|\downarrow\rangle$), leaving it unaffected otherwise. The topological invariants depend on the rotation angles θ_1 and θ_2, and are well known for both translationally invariant [49,50] and spatially disordered angles [21,51]. The chiral symmetry operator is $\hat{\Gamma} = \hat{1} \otimes \sigma_x$, so that the two sublattices correspond to the two internal states $|\pm\rangle = (|\uparrow\rangle \pm |\downarrow\rangle)/\sqrt{2}$. The particle starts in $|x = 0\rangle \otimes |-\rangle$; after each unitary step, we remove it if it occupies the state $|+\rangle$ [52], and record its position. Experimentally, a spin-selective removal of the particles can be achieved with long spin-dependent shift operations [38,47], followed by fluorescence imaging to record the position of the removed particles [48]. This realizes a strong measurement, $p_M = 1$, represented by the operator $\hat{M} = \hat{1} \otimes |-\rangle\langle -|$.

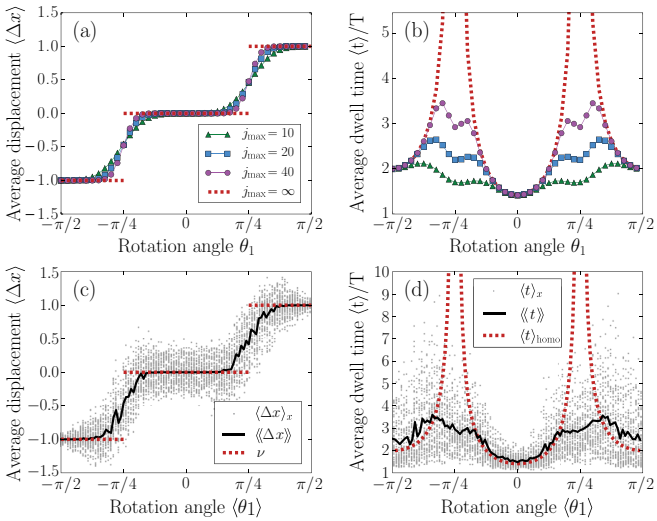

FIG. 3. Average displacement and dwell time for the split-step quantum walk with strong measurement ($p_M = 1$) as the coin angle θ_1 is tuned (θ_2 centered at $\pi/4$, $L = 50$ sites). Step changes of the average displacement indicate topological phase transitions. (a), (b) A homogeneous split-step walk with the time evolution terminated after $j_{\max}$ steps. (c), (d) Split-step walk with disordered rotation angles uniformly distributed in intervals of width $\pi/5$ (see text), with a total number of steps $j_{\max} = 40$. Black dots correspond to different initial sites, and the red curve represents their average.

The average displacement and the average dwell time are shown in Fig. 3 for numerical examples, both with and without spatial disorder. In the translationally invariant case, for parameters far from topological phase transitions, ten steps are sufficient to observe the quantized displacement predicted by Eq. (16) [53]. Close to a phase transition, the average dwell time becomes large, according to Eq. (17), and the quantization of the displacement breaks down if the particle is observed only for a finite number of steps. In the disordered case we use rotation angles chosen uniformly from the intervals $\theta_{1,2} \in [\langle\theta_{1,2}\rangle - \pi/10, \langle\theta_{1,2}\rangle + \pi/10]$. While the displacements for different initial states are no longer quantized, their average yields the quantized winding number, for time evolution terminated after 40 steps.

Discussion and conclusions. We proved that losses can be used to detect bulk topological invariants in chiral symmetric one-dimensional lattices, with any number of internal states, disordered or translationally invariant, periodically driven or static. This is a powerful generalization of some of the results of Rudner and Levitov on the SSH model; as in their case, we expect that it should even be possible to relax the requirement of chiral symmetry and allow for certain types of decoherence [25,54]. This approach should also be useful to obtain (weak) topological invariants of chiral symmetric systems in two dimensions and above. Exploring the relations between our results and the inspiring recent work by Cardano *et al.* [43,55] on the periodically driven SSH model would be an interesting topic for future research.

Acknowledgments. We acknowledge useful discussions with Mark Rudner. J.K.A. acknowledges support from the

Hungarian Scientific Research Fund (OTKA) under Contract No. NN109651, and from the Janos Bolyai Scholarship of the Hungarian Academy of Sciences. A.A. also acknowledges financial support from the the ERC grant DQSIM and from the Deutsche Forschungsgemeinschaft SFB/TR 185 OSCAR.

[1] M. Z. Hasan and C. L. Kane, Rev. Mod. Phys. **82**, 3045 (2010).
[2] J. C. Budich and B. Trauzettel, Phys. Status Solidi **7**, 109 (2013).
[3] C.-K. Chiu, J. C. Y. Teo, A. P. Schnyder, and S. Ryu, Rev. Mod. Phys. **88**, 035005 (2016).
[4] S. Ryu, A. P. Schnyder, A. Furusaki, and A. W. Ludwig, New J. Phys. **12**, 065010 (2010).
[5] J. C. Y. Teo and C. L. Kane, Phys. Rev. B **82**, 115120 (2010).
[6] V. Mourik, K. Zuo, S. M. Frolov, S. Plissard, E. Bakkers, and L. Kouwenhoven, Science **336**, 1003 (2012).
[7] A. J. Heeger, Rev. Mod. Phys. **73**, 681 (2001).
[8] H. M. Price, O. Zilberberg, T. Ozawa, I. Carusotto, and N. Goldman, Phys. Rev. B **93**, 245113 (2016).
[9] G. Jotzu, M. Messer, R. Desbuquois, M. Lebrat, T. Uehlinger, D. Greif, and T. Esslinger, Nature (London) **515**, 237 (2014).
[10] M. Aidelsburger, M. Lohse, C. Schweizer, M. Atala, J. T. Barreiro, S. Nascimbène, N. Cooper, I. Bloch, and N. Goldman, Nat. Phys. **11**, 162 (2015).
[11] N. Fläschner, B. Rem, M. Tarnowski, D. Vogel, D.-S. Lühmann, K. Sengstock, and C. Weitenberg, Science **352**, 1091 (2016).
[12] T. Li, L. Duca, M. Reitter, F. Grusdt, E. Demler, M. Endres, M. Schleier-Smith, I. Bloch, and U. Schneider, Science **352**, 1094 (2016).
[13] M. Leder, C. Grossert, L. Sitta, M. Genske, A. Rosch, and M. Weitz, Nat. Commun. **7**, 13112 (2016).
[14] E. J. Meier, F. A. An, and B. Gadway, Nat. Commun. **7**, 13986 (2016).
[15] M. Hafezi, S. Mittal, J. Fan, A. Migdall, and J. Taylor, Nat. Photonics **7**, 1001 (2013).
[16] J. M. Zeuner, M. C. Rechtsman, Y. Plotnik, Y. Lumer, S. Nolte, M. S. Rudner, M. Segev, and A. Szameit, Phys. Rev. Lett. **115**, 040402 (2015).
[17] F. Bleckmann, S. Linden, and A. Alberti, arXiv:1612.01850.
[18] C. Poli, M. Bellec, U. Kuhl, F. Mortessagne, and H. Schomerus, Nat. Commun. **6**, 6710 (2015).
[19] M. Atala, M. Aidelsburger, J. T. Barreiro, D. Abanin, T. Kitagawa, E. Demler, and I. Bloch, Nat. Phys. **9**, 795 (2013).
[20] I. C. Fulga, F. Hassler, and A. R. Akhmerov, Phys. Rev. B **85**, 165409 (2012).
[21] B. Tarasinski, J. K. Asbóth, and J. P. Dahlhaus, Phys. Rev. A **89**, 042327 (2014).
[22] I. C. Fulga and M. Maksymenko, Phys. Rev. B **93**, 075405 (2016).
[23] W. Hu, J. C. Pillay, K. Wu, M. Pasek, P. P. Shum, and Y. D. Chong, Phys. Rev. X **5**, 011012 (2015).
[24] S. Barkhofen, T. Nitsche, F. Elster, L. Lorz, A. Gabris, I. Jex, and C. Silberhorn, arXiv:1606.00299.
[25] M. S. Rudner and L. S. Levitov, Phys. Rev. Lett. **102**, 065703 (2009).
[26] J. K. Asbóth, L. Oroszlány, and A. Pályi, in *A Short Course on Topological Insulators: Band Structure and Edge States in One and Two Dimensions*, Lecture Notes in Physics Vol. 919 (Springer, Berlin, 2016).
[27] C. Bardyn, M. Baranov, C. Kraus, E. Rico, A. İmamoğlu, P. Zoller, and S. Diehl, New J. Phys. **15**, 085001 (2013).
[28] J. C. Budich, P. Zoller, and S. Diehl, Phys. Rev. A **91**, 042117 (2015).
[29] If the number of internal states involved in the system's dynamics is odd, it is not possible to have a system that is both chiral symmetric and gapped.
[30] In fact, we could relax the above condition and replace it with the less strict requirement $\hat{\Gamma}\hat{U}\hat{\Gamma} = \hat{U}^{\dagger}$, which is implied by Eq. (3).
[31] I. Mondragon-Shem, T. L. Hughes, J. Song, and E. Prodan, Phys. Rev. Lett. **113**, 046802 (2014).
[32] See Supplemental Material at http://link.aps.org/supplemental/10.1103/PhysRevB.95.201407 for details of the mathematical derivations of our main results.
[33] R. Resta, Phys. Rev. Lett. **80**, 1800 (1998).
[34] E. Prodan, J. Phys. A **44**, 113001 (2011).
[35] N. Goldman and J. Dalibard, Phys. Rev. X **4**, 031027 (2014).
[36] F. Zähringer, G. Kirchmair, R. Gerritsma, E. Solano, R. Blatt, and C. F. Roos, Phys. Rev. Lett. **104**, 100503 (2010).
[37] M. Karski, L. Förster, J.-M. Choi, A. Steffen, W. Alt, D. Meschede, and A. Widera, Science **325**, 174 (2009).
[38] C. Robens, W. Alt, D. Meschede, C. Emary, and A. Alberti, Phys. Rev. X **5**, 011003 (2015).
[39] A. Schreiber, K. N. Cassemiro, V. Potoček, A. Gábris, P. J. Mosley, E. Andersson, I. Jex, and C. Silberhorn, Phys. Rev. Lett. **104**, 050502 (2010).
[40] A. Peruzzo, M. Lobino, J. C. F. Matthews, N. Matsuda, A. Politi, K. Poulios, X.-Q. Zhou, Y. Lahini, N. Ismail, K. Wörhoff, Y. Bromberg, Y. Silberberg, M. G. Thompson, and J. L. O'Brien, Science **329**, 1500 (2010).
[41] T. Kitagawa, M. A. Broome, A. Fedrizzi, M. S. Rudner, E. Berg, I. Kassal, A. Aspuru-Guzik, E. Demler, and A. G. White, Nat. Commun. **3**, 882 (2012).
[42] L. Sansoni, F. Sciarrino, G. Vallone, P. Mataloni, A. Crespi, R. Ramponi, and R. Osellame, Phys. Rev. Lett. **108**, 010502 (2012).
[43] F. Cardano, A. D'Errico, A. Dauphin, M. Maffei, B. Piccirillo, C. de Lisio, G. De Filippis, V. Cataudella, E. Santamato, L. Marrucci *et al.*, arXiv:1610.06322.
[44] E. Flurin, V. V. Ramasesh, S. Hacohen-Gourgy, L. S. Martin, N. Y. Yao, and I. Siddiqi, arXiv:1610.03069.
[45] V. V. Ramasesh, E. Flurin, M. S. Rudner, I. Siddiqi, and N. Y. Yao, Phys. Rev. Lett. **118**, 130501 (2017).
[46] T. Groh, S. Brakhane, W. Alt, D. Meschede, J. K. Asbóth, and A. Alberti, Phys. Rev. A **94**, 013620 (2016).
[47] C. Robens, W. Alt, C. Emary, D. Meschede, and A. Alberti, Appl. Phys. B **123**, 12 (2016).
[48] A. Alberti, C. Robens, W. Alt, S. Brakhane, M. Karski, R. Reimann, A. Widera, and D. Meschede, New J. Phys. **18**, 053010 (2016).
[49] T. Kitagawa, E. Berg, M. Rudner, and E. Demler, Phys. Rev. B **82**, 235114 (2010).
[50] J. K. Asbóth and H. Obuse, Phys. Rev. B **88**, 121406 (2013).

[51] T. Rakovszky and J. K. Asboth, Phys. Rev. A **92**, 052311 (2015).
[52] A basis change by $\pi/2$ microwave pulses is required to selectively remove $|-\rangle$.
[53] We checked that the plateaus seen in Fig. 3 remain observable also in the presence of sufficiently weak dephasing processes of the kind discussed in Ref. [56]. We expect the average displacement to remain quantized also for a "jittering" of the timing of the measurement operation, provided chiral symmetry of the unitary evolution between two measurements is preserved.
[54] M. S. Rudner, M. Levin, and L. S. Levitov, arXiv:1605.07652.
[55] F. Cardano, M. Maffei, F. Massa, B. Piccirillo, C. de Lisio, G. De Filippis, V. Cataudella, E. Santamato, and L. Marrucci, Nat. Commun. **7**, 11439 (2016).
[56] A. Alberti, W. Alt, R. Werner, and D. Meschede, New J. Phys. **16**, 123052 (2014).